Effect of K substitution on Structural, Electrical and Magnetic Properties of Bi-2212 system

B. Özçelik[a*], M. Gursul[a], A. Sotelo[b], M. A. Madre[b]

[a]*Department of Physics, Faculty of Sciences and Letters, Çukurova University. 01330 Adana, Turkey*

[b]*ICMA (CSIC-Universidad de Zaragoza). María de Luna, 3. 50018 Zaragoza, Spain.*

Abstract

In this work, the effect of K in the $Bi_2Sr_2Ca_{1-x}K_xCu_2O_{8+y}$ superconductor with x=0.0, 0.05, 0.075, and 0.1, has been investigated. The samples were prepared by a polymer solution technique using polyethyleneimine, PEI. The effects of K substitution have been investigated by electrical resistivity (ρ-T), scanning electron microscopy (SEM), X-ray diffraction (XRD), energy dispersive X-ray spectroscopy (EDX), and magnetic characterizations. SEM and XRD have shown that the Bi-(2212) phase is the major one independently of the K content. Moreover, the microstructure of samples is improved with K content up to x=0.075. Electrical resistivity measurements have found that *Tc* is slightly higher than 91 K for K contents up to 0.075, decreasing for higher doping in only about 0.5 K. Moreover, this trend is maintained in the magnetic measurements which have shown that the hysteresis loops are increased until 0.075 K contents. The maximum calculated *Jc*, using Bean's model, has been of around 4.5 10^6 A/cm^2 at 10 K and ~ 1000 Oe for the 0.05 K doped samples.

Keywords: Bi-based cuprates, XRD, SEM, Critical Current, M-H

***Corresponding Author:** Tel./fax:+90.322.3386060/2496/+90.322.3386070
e-mail: ozcelik@cu.edu.tr

1. Introduction

Since the discovery of high-*Tc* superconductivity in Bi-based high-temperature superconductors (HTSC) [1], which provides the most promising materials for potential technological and industrial applications [2–4], intense studies have been performed [5-18] in order to improve its critical temperature (*Tc*), critical current density (*Jc*), and better understand the structural properties of the system. As it is well-known, the Bi-based superconductor family comprises three different phases which can be described by the $Bi_2Sr_2Ca_{n-1}Cu_nO_{2n+4+y}$ general formula, where n =1, 2 and 3. Moreover, n is related to the number of CuO_2 layers in the crystal structure, producing the Bi-2201, 2212 and 2223, respectively, with 20, 85, and 110 K critical temperatures, respectively [19-21]. For many years, researchers have tried to improve their structural, mechanical and superconducting properties by using several techniques [13–21]. Especially, one of the most useful methods to improve the physical properties, in this regard, is the substitution of some elements at different cationic sites. These substitutions lead to important changes in charge carrier concentration and also release the restriction of spin alignment due to the spin lattice interaction [22]. The effect of such changes is one of the important features that help understanding the structural details and superconducting properties along with the mechanism of occurrence of superconductivity [23-25]. Besides chemical doping, the synthetic methods have also been widely studied by researchers to produce high quality and homogeneous samples. Among these preparation techniques, some of them can be underlined, as the classical solid state [26,27] melt quench [28-31], sol-gel [32-35] and the polymer matrix [36-38] methods.

The aims of the present work are: **(*i*)** introducing optimum amounts of K into the $Bi_2Sr_2Ca_{1-x}K_xCu_2O_{8+y}$ system by replacing Ca, **(*ii*)** exploring the structural, electrical and magnetical behavior of the modified systems **(*iii*)** evaluating the results as a function of K content. In previous works, the effects of several substitutions for Ca or Cu have been estudied [39-42]. In the framework of this study, the modification of Bi-2212 ceramics physical properties induced by the K substitution for Ca has been determined by means of X-ray analysis (XRD), scanning electron microscopy (SEM), electron dispersive X-ray (EDX), and magnetic measurements.

2. Experimental details

$Bi_2Sr_2Ca_{1-x}K_xCu_2O_y$ samples, with x =0, 0.05, 0.075 and 0.1 have been prepared, by using a polymer matrix route described in detail elsewhere [16,43]. $Bi(CH_3COO)_3$ (≥99.99%,

Aldrich), $Sr(CH_3COO)_2 \bullet 0.5H_2O$ (99%, Panreac), $Ca(CH_3COO)_2 \bullet 2H_2O$ (98%, Alfa Aesar), $Cu(CH_3COO)_2 \bullet H_2O$ (98%, Panreac) and $K(CH_3COO)$ (99%, Alfa Aesar) commercial powders were used as starting materials. They were weighed in stoichiometric amounts and dissolved in a mixture of glacial acetic acid (CH_3COOH) (Panreac PA) and distilled water. The use of a mixture of glacial acetic acid and water is due to the fact that in one side Sr acetate is insoluble in concentrated acetic acid and, on the other side; Bi acetate is not soluble in water [44]. Once obtained a clear blue solution, polyethyleneimine (PEI) (Aldrich, 50 wt.% water) solution in distilled water, in order to reduce the viscosity of commercial PEI, was added. The mixture becomes dark blue immediately reflecting the formation of Cu-N coordination bonds. The solution was then introduced into a rotary evaporator to reduce its volume (in ~80%) followed by heating on a hot plate at about 100 ºC for total solvent evaporation, producing a thermoplastic dark blue paste. Further heating at around 350 ºC produces a decomposition step, as described schematically elsewhere [37], which produces the organic material decomposition. The resulting powder was then milled in an agate mortar and calcined twice at 750 and 800°C for 12 h in order to decompose the alkaline-earth carbonates, avoiding the bubbles formation in the subsequent melting process.

Finally, the prereacted homogeneous powders were pressed into pellets with 13 mm in diameter, and thermally treated in order to produce the Bi-2212 superconducting phase. This process was performed under air, and consisted in two steps: 60 h at 860 ºC, followed by 12 h at 800 ºC and, finally, quenched in air to room temperature.

In order to identify the present phases, powder X-ray diffraction patterns of the materials were recorded at room temperature using a Rigaku D/max-B powder diffractometer system working with CuKα radiation and a constant scan rate between 2θ= 3-80º. The uncertainty of the crystal lattice parameters calculation remained in the ± 0.00001 range. SEM micrographs were taken using a LEO Evo-40 VPX scanning electron microscope (SEM) fitted with an energy dispersive spectrometry (EDS) analysis system. Magnetic measurements were carried out in a Quantum Design PPMS system. The $Bi_2Sr_2Ca_{1-x}K_xCu_2O_{8+y}$ samples, with x =0, 0.05, 0.075, and 0.1will be hereafter named as A, B, C and D, respectively

3. Results and discussion

3.1 XRD characterization

The normalized XRD patterns obtained for all the samples are presented in Fig.1 where the peaks for the Bi-2212 superconducting phase have been indicated by #2 [42]. From these graphs, it can be seen that both pure and K-doped samples contain the Bi-2212 phase as the major one, independently of the amount of the K doping. Moreover, small amounts of $CaCuO_2$ nonsuperconducting secondary phase (indicated by *) can be detected in all the samples, which is a clear indication that K does not destabilizes the Bi-2212 superconducting phase. From the XRD data, it has been determined that the crystal symmetry of all the samples is tetragonal and the lattice parameters were calculated using the least squares method and then presented in Table 1. As it can be inferred from these data, while *a-b* parameters are slightly increasing, c-parameter is decreasing when increasing K content is raised. It is argued that the variation of the oxygen content on the lattice structure by substituting K for Ca ions can cause the reduction in the *c*-parameter and, consequently, the raise in the *a-b* parameters.

In order to get more information about the crystal sizes, the Debye Scherer formula [45] has been applied to the XRD data, as:

$$L_{hkl} = 0{,}9\,\lambda / \beta\cos\theta \qquad (1)$$

where λ is the used wavelength, β is the full width at half maximum and θ is the angle of the peak. As can be seen from Table 1, the particle sizes increase with increasing K-content, up to x=0.075.

3.2 SEM analysis

The surface morphologies of all samples have been observed with SEM and the micrographs are displayed in Fig. 2. From these images, it can be clearly seen that the surface morphology of the A, B, and D samples are very similar. These samples are formed by randomly oriented closely packed and dense plate-like grains together with some porosity. On the other hand, C samples have a more uniform surface with a dense alignment of plate-like grains. In addition, with the increasing of K, the porosity of the samples slightly decreases when K is added until an optimum value of 0.075. Further K additions produce a deterioration of microstructure and, in fact, the amount of porosity increases in an important manner.

3.3 Electrical measurements

The electrical resistivity (ρ) versus temperature (T) curves obtained for all samples are plotted in Fig. 3 from 150 K down to 60 K. In this figure, it can be clearly seen that samples A, B, C and D possess a very similar behavior over the onset critical temperature (T_c^{onset}) transition, with a metallic-like behavior. Under the superconducting T_c^{onset} transition temperatures, the *ρ(T)* curves show typical characteristics of common Bi-2212 superconductors in all tested samples, which have a relatively sharp decreasing after T_c^{onset} transition temperatures. On the other hand, the offset transition temperature (T_c^{offset}) values slightly increase with raising K concentration (see Table 1). This trend in transition temperature values indicates the improved superconducting properties of the system with increasing K concentration. In addition, the T_c^{onset} transition temperature value was found to be almost unchanged compared with pure sample. It reveals small changes in hole concentration values calculated from Presland equation [46] (see Table 1). The onset and offset critical temperatures obtained from the normalized resistivity graph versus temperature are tabulated in Table 1. It can be easily seen that T_c^{onset} gradually decrease with the increase of K amount, but T_c^{offset} increases up to x=0.075 K. Additionally, the difference between onset and offset critical temperatures is decreased with the decreasing of K content up to x=0.075, indicating a higher slope in the transition between the normal to the superconducting state.

3.4 Magnetic properties

The magnetic-hysteresis cycles, between applied fields of ± 9 kOe, for all the samples, at 10, 20, and 30 K are shown in Fig. 4. The magnetic-hysteresis loops of the samples shows that the magnitude of magnetization effectively depends on K doping levels. There is a clear raise of magnetization volume in the entire range of magnetic fields for all samples when K content is increased, except for samples D, *i.e.* the hysteresis loops are getting larger with increasing doping K-content while they decrease when temperature is increased. In addition, the diamagnetic behavior observed in the M-H loops of all samples except for x = 0.1 sample confirms the occurrence of a conventional type-II superconductors. These effects can be explained using the arguments described previously in the electrical measurements section. Moreover, they are confirmed with the SEM observations which show an increase of the K-substituted Bi-2212 phase when K content is raised. As a consequence of the higher amount of the K-doped phase up to x=0.075, the superconducting properties of these samples are improved. Further K doping increases the Cooper pair breaking and the magnetic properties diminished.

From these magnetic data, the *Jc* values of the samples were determined using the Bean's model [47];

$$Jc = 30 \Delta M / d \qquad (2)$$

where *Jc* is the magnetization current density in ampéres per square centimeter of a sample. $\Delta M = M+ - M-$ is measured in electromagnetic units per cubic centimeter, and *d* is the thickness of sample.

Figure 5 shows the critical current density value at 10 K estimated from M-H loops for all samples up to 1 T. Calculated *Jc* of all samples effectively increases with the increasing of magnetic field and K contents up to 0.1 T, then starts to decrease. The important raise in the *Jc* values for the K-doped samples studied in this work up to x=0.075 implies that the resistance to the flux creep of those samples are smaller than that of the others due to the higher superconducting properties of K-substituted Bi-2212 phases which do act as effective pinning centers. It can be also concluded that the field dependence of J_C above 0.1 T can be related to the presence of structural defects or the weak links between grains, typical feature in ceramic superconductors.

The temperature dependence of ZFC magnetizations of the samples has been measured and displayed in Fig. 6, under an external applied magnetic field of 50 Oe. In the zero field cooled (ZFC) phase the samples become diamagnetic below their onset temperatures and diamagnetic saturation is almost reached at the lowest temperatures. Additionally, it can be concluded that the magnetizations show an incremental tendency on the superconducting properties with the raise of K-content up to x=0.05. Then the magnetization of the samples starts to decrease pointing out the lower superconducting properties in the samples. These behaviors are mainly caused by their granular nature, together with the effect of the weak connectivity at the grain boundaries.

3.5 Conclusions

In this study, we aim to improve the microstructural, electrical and superconducting properties of the BSCCO superconducting ceramics prepared by a polymer matrix route by partial replacement of K for Ca in its crystal structures. The well-known experimental techniques such as the X-ray diffraction, scanning electron microscopy, dc-resistivity and dc-magnetization and magnetic hysteresis are performed to find the optimum doping level of K-

content. The whole results point out that the characteristics above mentioned improve regularly with the raise of the K-content up to a critical value of x=0.075 after which the superconducting properties tend to decrease. XRD suggests that samples with nearly single Bi-2212 phase have been obtained, independently of the K content. The SEM micrographs confirm that all samples are predominantly composed by randomly oriented plate-like grains of the Bi-2212 phase. R-T results indicated that all samples exhibit metallic behavior over T_c^{onset}. Moreover, all of them showed a broad transition from the normal to the superconducting state, pointing out to the presence of impurities and weak links between superconducting grains, except for the C samples. From M-H measurements, it has been found that the magnetization values and the volume of the closed hysteresis curves increase with increasing K-content up to x=0.075, due to the formation of the K-substituted Bi-2212 phase. Employing Bean's model, it has been found that the increase on K contents produces a increase on *Jc* values, again up to x=0.075.

Acknowledgements

This work is supported by Research Fund of Cukurova University, Adana, Turkey, under grant contracts no: FEF 2013YL17 and FEF2013BAP22.

References

[1] H. Maeda, Y. Tanaka, M. Fukutomi, T. Asano, Jpn. J. Appl. Phys. 27, L209 (1988)

[2] S.Y.Oh, H.R.Kim, Y.H. Jeong, O.B. Hyun, C.J Kim, Physica C **463–465**, 464 (2007)

[3] M.Chen, W. Paul, M. Lakner, L. Donzel, M. Hoidis, P. Unternaehrer, R.Weder, M.Mendik, Physica C **372**, 1657 (2002)

[4] J.D. Hodge, H. Muller, D.S. Applegate, Q. Huang, Appl. Supercond. **3**, 469 (1995)

[5] A. Coskun, A. Ekicibil, B. Ozcelik, Chin.Phys.Lett. 19/12, 1863 (2002)

[6] D. Yazıcı, B. Ozçelik, M.E. Yakıncı, J. Low Temp. Phys. 163, 370 (2011)

[7] A. Sotelo, M. Mora, M. A. Madre, J. C. Diez, L. A. Angurel, G. F. de la Fuente, J. Eur. Ceram. Soc. 25, 2947 (2005)

[8] L. Jiang, Y. Sun, X. Wan, K. Wang, G. Xu, X. Chen, K. Ruan, J. Du: Physica C 300, 61 (1998)

[9] M. Zargar Shoushtari, S. E. Mousavi Ghahfarokhi: J.. Supercond. Nov. Magn. 24, 1505 (2011)

[10] A. I. Abou-Aly, M.M.H. Abdel Gawad, R. Awad, I. G-Eldeen: J. Supercond. Nov. Magn. 24, 2077 (2011)

[11] M. Mora, A. Sotelo, H. Amaveda, M. A. Madre, J. C. Diez, L. A. Angurel, G. F. de la Fuente, Bol. Soc. Esp. Ceram. V. 44, 199 (2005)

[12] A. Sotelo, M. A. Madre, J. C. Diez, Sh. Rasekh, L. A. Angurel, E. Martinez, Supercond. Sci. Technol. 22, 034012 (2009)

[13] M. A. Madre, H. Amaveda, M. Mora, A. Sotelo, L. A. Angurel, J. C. Diez, Bol. Soc. Esp. Ceram. V. 47, 148 (2008)

[14] Y.L. Chen, R. Stevens: J. Am. Ceram. Soc. 75, 1150 (1992)

[15] R. Ramesh, S. Green, C. Jiang, Y. Mei, M. Rudee, H. Luo, G. Thomas: Phys. Rev. B, Condens. Matter 38, 7070 (1988)

[16] G. F. de la Fuente, A. Sotelo, Y. Huang, M. T. Ruiz, A. Badia, L. A. Angurel, F. Lera, R. Navarro, C. Rillo, R. Ibañez, D. Beltran, F. Sapiña, A. Beltran, Physica C 185, 509 (1991)

[17] A. Sotelo, H. Szillat, P. Majewski, F. Aldinger, Supercond. Sci. Technol. 10, 717 (1997)

[18] B. Özkurt, M. A. Madre, A. Sotelo, M.E. Yakıncı, B. Özçelik, J. Supercond. Nov. Magn. 25, 799 (2012)

[19] L.Gao, J. C. Huang, L. R. Meng, H. P. Hor, J.Bechtold, Y.Y. Sun, W. C. Chu, Z.Z. Sheng, M. A. Herman,: Nature 332, 623 (1988)

[20] W.C. Chu, J.Bechtold, L.Gao, H.P. Hor, J.C. Huang, L.R. Meng, Y.Y. Sun, Y.Q.Wang, Y.Y.Zue: Phys. Rev. Lett. 60,941 (1988)

[21] L.J. Tallon, G.R. Buckley, W.P.Gilbert, R.M.Presland, M.W.I. Brown, E.M. Bowder, A.L. Christian, R.Gafull: Nature 333, 153 (1988)

[22] Y. Ando, A.N. Lavrov, S. Komiya, K. Segawa, X.F. Sun: Phys. Rev. Lett. 87:017001 (2001)

[23] J.M. Tarascon, P. Barboux, G.W. Hull, R. Ramesh, L.H. Greene, M. Gariod, M.S. Hedge, W. R. Mckinnon: Phys. Rev. B 38, 4316 (1989)

[24] H. Eisaki, N. Kaneko, D. Feng, L. Fengi, A. Damascelli, P.K. Mang, Z.X. Shen, M. Greven:Phys. Rev. B 69, 064512 (2004)

[25] K. Fujita, T, Noda, K.M. Kojima, H. Eisaki, S. Uchida: Phys. Rev. Lett. 95, 097006 (2005)

[26] N. Knauf, J. Harwischmacher, R. Miller, R. Borowski, B. Rodeu, D. Wohllebreu, Physica C 173, 414 (1991)

[27] M. F. Carrasco, F. M. Costa, R. F. Silva, F. Gimeno, A. Sotelo, M. Mora, J. C. Diez, L. A. Angurel, Physica C 415, 163 (2004)

[28] S. Elschner, J. Boch, G. Brommer, P. Hermann, IEEE Trans. Magn. 21, 2724 (1996)

[29] N. Türk, H. Gündogmus, M. Akyol, Z. D. Yakıncı, A. Ekicibil, B. Özçelik, J.Supercond. Nov. Magn 27, 711 (2014)

[30] D. Yazici, B. Ozcelik, J. Supercond. Nov. Magn., 25, 293 (2012)

[31] D. Yazıcı, B. Ozcelik, S. Altın, M. E. Yakıncı, J.Supercond.Nov. Magn.,24, 217 (2011)

[32] C. J. Huang, T.Y. Tseng, T. S. Heh, F. H. Chen, W. S. Jong, Y. S. Fran, S. M. Shiau, Solid State Commun. 72, 563 (1989)

[33] R.S. Liu, W.N. Wang, C.T. Chang, P.T. Wu, Jpn. J. Appl. Phys. 28, L2155 (1989)

[34] T. Asaka, Y. Okazawa, T. Hirayama, K. Tachikawa, Jpn. J. Appl. Phys. 29, L280 (1990)

[35] A. Sotelo, M. A. Madre, Sh. Rasekh, J. C. Diez, L. A. Angurel, Adv. Appl. Ceram. 108, 285 (2009)

[36] A. Sotelo, G. F. de la Fuente, F. Lera, D. Beltran, F. Sapiña, R. Ibañez, A. Beltran, M. R. Bermejo, Chem. Mater. 5, 851 (1993)

[37] A. Sotelo, L. A. Angurel, M. T. Ruiz, A. Larrea, F. Lera, G. F. de la Fuente, Solid State Ionics 63, 883 (1993)

[38] A. Sotelo, J. I. Peña, L. A. Angurel, J. C. Diez, M. T. Ruiz, G. F. de la Fuente, R. Navarro, J. Mater. Sci. 32, 5679 (1997)

[39] D. Yazıcı, B. Ozcelik, S. Altın, M. E.Yakıncı, J.Supercond. Nov. Magn.,24, 217 (2011)

[40] H. Gündogmus, B. Özçelik, B. Özkurt, A. Sotelo, M.A. Madre, J. Supercond. Nov. Magn, 26, 111(2013)

[41] A. Ozaslan, B. Özçelik, B. Özkurt, A. Sotelo, M.A. Madre, J. Supercond. Nov. Magn, 27, 53 (2014)

[42] C. Kaya, B. Özçelik, B. Özkurt, A. Sotelo, M.A. Madre, J Mater Sci:Mater Electron, 24, 1580 (2013)

[43] A. Sotelo, Sh. Rasekh, M.A. Madre, J.C. Diez: J. Supercond. Nov. Magn. 24, 19 (2011)

[44] D.R. Lide: CRC Handbook of Chemistry and Physics. CRC Press/Taylor and Francis, Boca Raton, FL (2010)

[45] B. D. Cullity, Element of X-ray Differaction, Addition-Wesley, Reading, MA (1978)

[46] M.R. Presland, J.L. Tallon, R.G. Buckley, R.S. Liu, N.E. Floer, Physica C **176**, 95 (1991)

[47] C.P. Bean, Phys. Rev. Lett. 8, 250 (1962)

Table 1. T_c values deduced from the R-T measurement data, unit cell parameters, crystal size and hole-carrier concentration for each type of samples.

Samples	***T_c(K)***	***ΔT(K)***	***Unit-cell parameter a=b (Å)***	***Unit-cell parameter c (Å)***	***L_{hkl}* (Å)**	***Hole Concentration (p)***
A	**T_c^{onset} =91.43 $T_{c.}^{offset}$=80.01**	**11.42**	5.3893	30.8657	375.6	**0.1333**
B	**$T_{c.}^{onset}$=91.40 $T_{c.}^{offset}$=80.13**	**11.27**	5.4053	30.8542	385.96	**0.1336**
C	**$T_{c.}^{onset}$=91.36 $T_{c.}^{offset}$=82.38**	**8.98**	5.4141	30.8276	398.42	**0.1406**
D	**$T_{c.}^{onset}$=90.77 $T_{c.}^{offset}$=76.76**	**14.01**	5.4183	30.7306	394.14	**0.1257**

Figure captions

Figure 1. XRD patterns of the A, B, C, and D samples. Peaks corresponding to the Bi-2212 and $CaCuO_2$ phases are indicated by #2 and *, respectively.

Figure 2. SEM micrographs of the $Bi_2Sr_2Ca_{1-x}K_xCu_2O_y$ (x= 0, 0.05, 0.1 and 0.25) samples.

Figure 3. The dc electrical resistivity versus temperature curves for all samples between 60 and 150 K.

Figure 4. M-H curves for all samples measured at 10, 20 and 30 K

Figure 5. Calculated critical current densities, J_c, of the samples, as a function of the applied field, at 10K.

Figure 6. Magnetization against temperature for samples at an applied field of 50 Oe

Figure 1

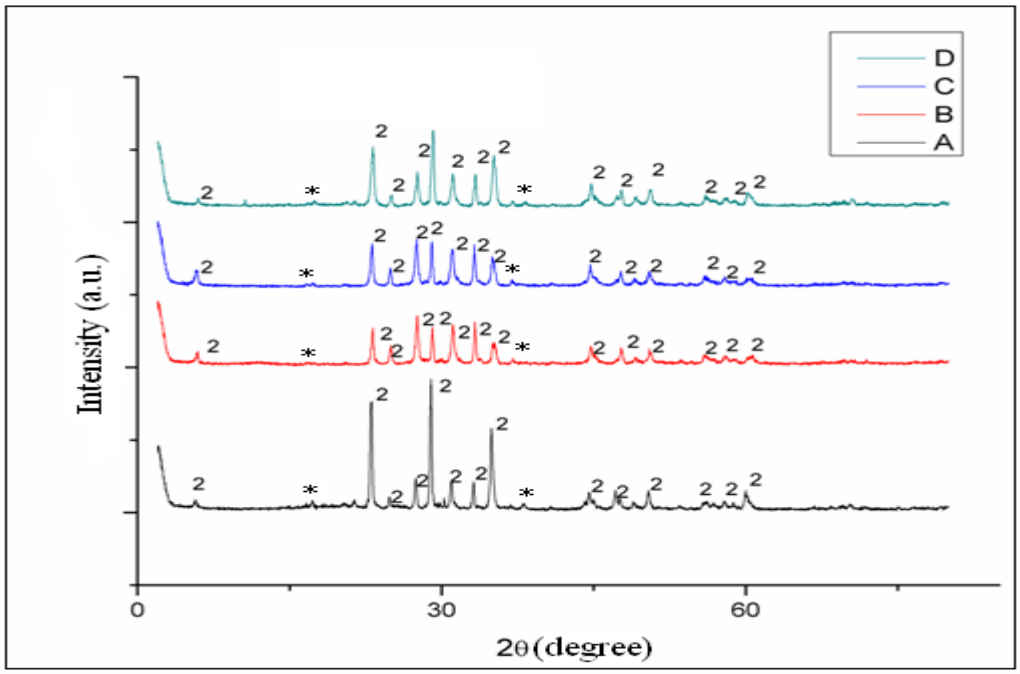

Figure 2

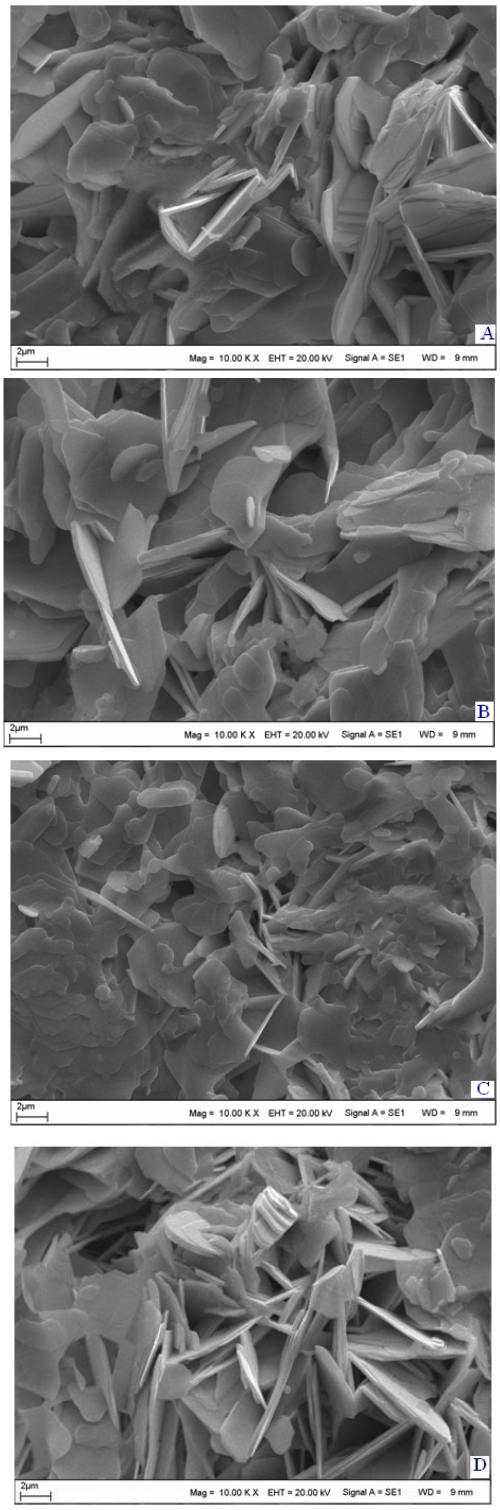
A
2µm
Mag = 10.00 K X EHT = 20.00 kV Signal A = SE1 WD = 9 mm
B
2µm
Mag = 10.00 K X EHT = 20.00 kV Signal A = SE1 WD = 9 mm
C
2µm
Mag = 10.00 K X EHT = 20.00 kV Signal A = SE1 WD = 9 mm
D
2µm
Mag = 10.00 K X EHT = 20.00 kV Signal A = SE1 WD = 9 mm

Figure 3

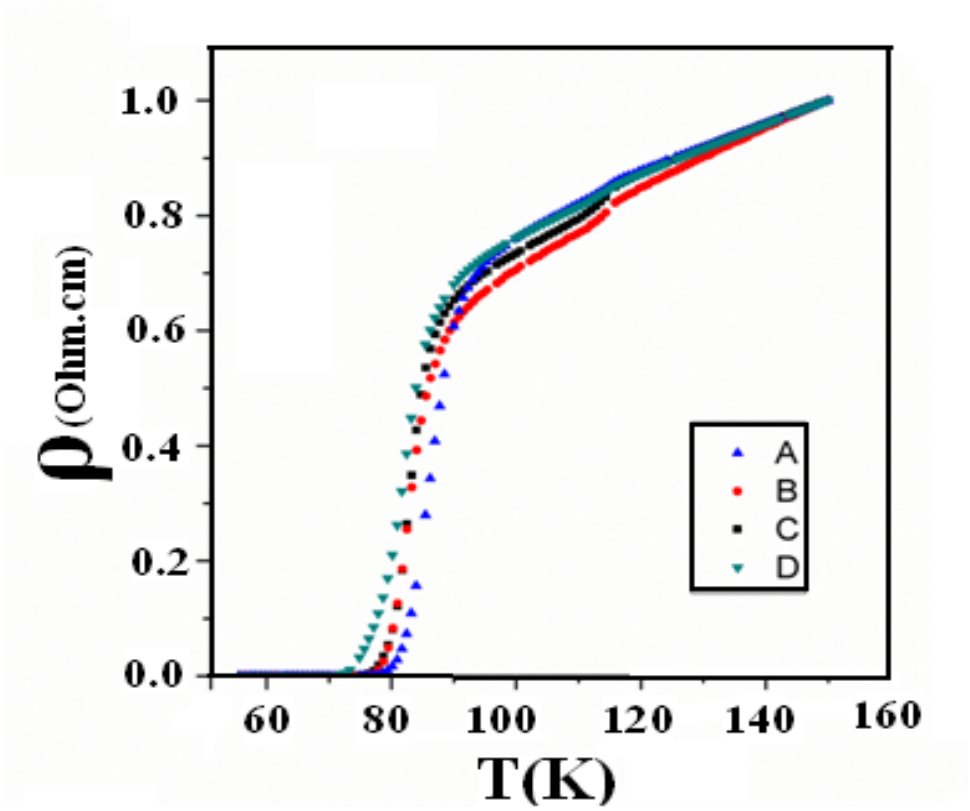

Figure 4

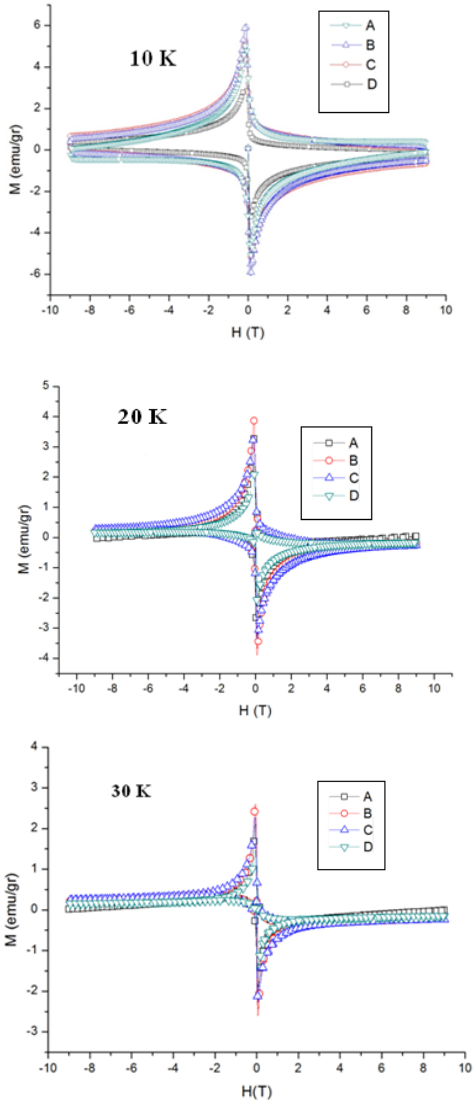

Figure 5

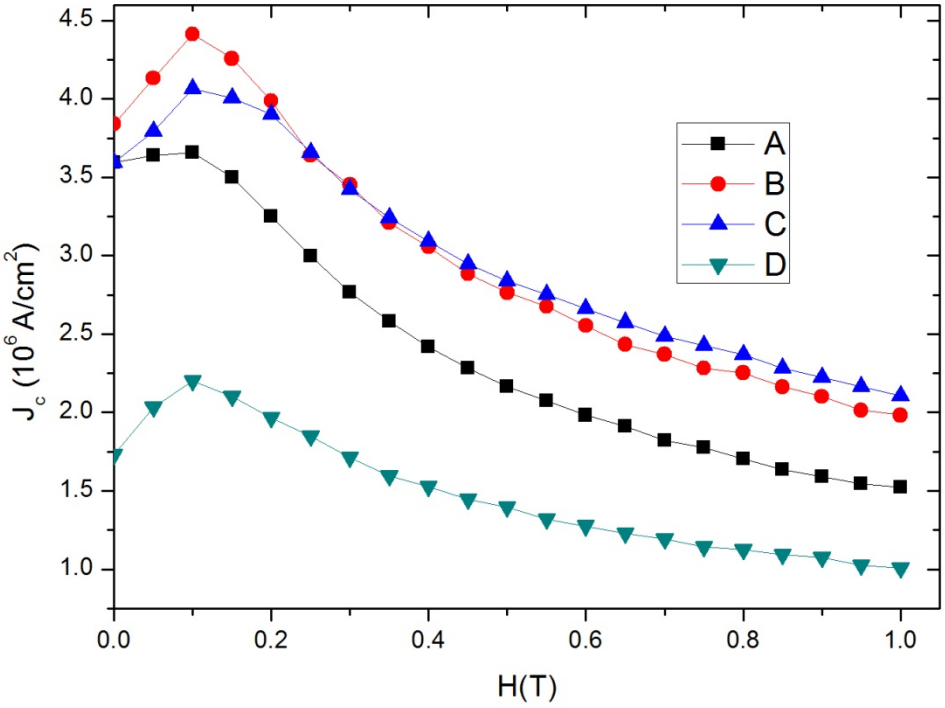

Figure 6